Int J Thermophys (2007) 28:2176–2187
DOI 10.1007/s10765-007-0245-4

High-Temperature Metallic Melts – Resistivity Intercomparison for Space Applications

C. Cagran · T. Hüpf · G. Pottlacher · G. Lohöfer

Published online: 13 September 2007
© Springer Science+Business Media, LLC 2007

Abstract Liquid state densities and electrical resistivities of pure copper and nickel as well as some of their binary alloys in the vicinity of the constantan mixing ratio (Cu53Ni47 at%) were measured by electromagnetic levitation and pulse-heating techniques. The experiments were performed as part of a joint project between the German Aerospace Center (DLR) and Graz University of Technology (TUG) with the main objective being to compare and support deeper understanding of different techniques for electrical resistivity measurements and their data. The manufacture of a levitation experiment similar to the setup at DLR is underway, which is scheduled for microgravity (μg) experiments onboard the ISS in 2010. As a first step, DLR performed measurements on a set of binary Cu–Ni-alloys (as well as two pure constituents), and independent experiments for constantan and the two pure metals were conducted at TUG. The results give promising agreement between the two techniques, show a reasonable overlap within the estimated uncertainties, and lead the way to more comparative measurements with newly developed materials.

Keywords Copper · Density · Electrical resistivity · High temperatures · Liquid state · Nickel

C. Cagran · T. Hüpf · G. Pottlacher (✉)
Institute of Experimental Physics, Graz University of Technology, Petersgasse 16, Graz 8010, Austria
e-mail: pottlacher@tugraz.at

G. Lohöfer
Institute of Materials Physics in Space, German Aerospace Center (DLR), 51147 Cologne, Germany

1 Introduction

The electrical resistivity of metals and alloys has proven to be of significant importance for many metal processing operations dealing with liquid materials. Casting processes or crystal growth furnaces (to name a few) are directly influenced by different melt flow due to electromagnetic fields and forces and thus dependent on the resistivity of the sample material.

Furthermore, knowledge of the temperature-dependent electrical resistivity allows calculation of the thermal conductivity using the Wiedemann–Franz relation. Although this procedure is generally limited to pure metals, earlier investigations indicated that this approach could also lead to very promising 'estimates' for alloys in the liquid state—or even in the solid state—if the phonon contribution to conduction is small. Electrical resistivity is also a sensitive indicator of structural changes (such as scattering of the free electrons at the positively charged core ions of the material) in the melt.

An ambitious joint project between the Institute of Materials Physics in Space, DLR, and Graz University of Technology, TUG, was initiated to respond to increased interest in electrical resistivity measurements and to advance current techniques. Roughly split into three major sections, the first phase of the project aims to evaluate and compare different resistivity measurement techniques, namely levitation and resistive pulse-heating, for metallic melts under 'normal' surface condition.[1] This first step is to compare and check the two techniques in terms of reproducibility and comparability as none of the techniques has been used with the main focus on resistivity measurements. Therefore, a full investigation and comparison of the two techniques is of great importance. Step 2 consists of in-flight microgravity experiments, tentatively scheduled for 2010 onboard the International Space Station, with candidate materials (metals and alloys) selected during Step 1. While DLR already has experience with microgravity surface tension and viscosity experiments [1], in-flight resistivity measurements are completely new ground for all project partners, resulting in the design of a new electromagnetic levitation device named MSL-EML, which is based on its predecessor TEMPUS [1], but with additional resistivity measurement capabilities [2]. Post-flight data evaluation and interpretation marks the last of the three planned steps during this project.

With the project currently in phase 1, measurements reported here are a comparison of density and electrical resistivity data for the metals copper and nickel as well as binary alloys made of these constituents.

Microgravity resistivity data for molten materials and undercooled melts will help to sort out any possible contributions deriving from electromagnetic or gravitational fields under 'normal' conditions, and are expected to increase measurement accuracy for future measurements, and to contribute to new high performance materials.

[1] The term 'normal' refers to conditions as present on earth's surface, e.g., gravitational forces and electromagnetic fields.

2 Measurements

To carry out such a comparison of electrical resistivity data for molten materials, measurements were performed with two different approaches: electromagnetic levitation at DLR and resistive pulse-heating at TUG. As only a comparison of electrical resistivity including thermal volume expansion is reasonable, the latter technique explicitly depends on a separate determination of thermal expansion. Keeping this in mind, a comparison of density data for the liquid samples obtained with both techniques will also be presented.

2.1 Levitation Setup

All measurements at DLR were performed with an electromagnetic levitation experiment, built into an ultra-high vacuum chamber. Lifting and heating of the sample is handled by the magnetic levitation field and induced currents. A variable stream of high purity argon mixed with helium is used to actively control the sample's temperature, especially to cool and further undercool the sample. The actual sample temperature is monitored by means of an infrared pyrometer. Although these preconditions are the same for the density and resistivity measurements, completely different experimental setups are employed due to different optical/electrical requirements.

For the density measurements, the levitated sample is backlit by an expanded He–Ne laser beam. The shadowgraph of the sample then passes a bandpass filter to get rid of possible stray light and is focused on a pinhole aperture to discriminate non-parallel beam components. Finally, it is recorded with a CCD camera and fed to a program running a real-time edge-detection algorithm. This procedure was designed and found to be insensitive to sample movements along the optical axes (e.g., apparent size changes) and to lateral sample movements, as long as the entire sample remains in the field-of-view (FOV). The entire optical setup needs to be calibrated with known and well-defined reference samples, e.g., precision ball bearings.

A completely different approach needs to be used for resistivity measurements. A measurement transformer (consisting of a primary and secondary coil) has to surround the levitated sample but be geometrically positioned between the levitation coils and the sample position. The primary transformer coil generates a high-frequency magnetic field, inducing a voltage in the secondary coil. This induced voltage depends on the sample's resistivity, its radius, its actual shape (deviation from spherical geometry) and allows the calculation of electrical resistivity if the system's calibration constants (which are dependent on the radius and the shape) are already known. Finally, to obtain the absolute resistivity, a calibration with perfectly spherical samples of known resistivity needs to be carried out. Schematics of all setups and more elaborate experimental descriptions of the experiments have been omitted to focus on the experimental comparisons. For more detailed information, interested readers are encouraged to consult Refs. [3] and [4].

2.2 Pulse-Heating Setup

Pulse-heating utilizes the passage of an intense current pulse over the conducting sample which results in resistive self-heating of the test material. In contrast to levitation techniques, pulse-heated samples can be brought from room temperature up to the end of the stable liquid phase in about 60 μs, usually collapse due to gravitational forces at the end of the experiment (or literally 'explode' due to increasing gas pressure at the boiling point), and thus can only be used once. However, in return, pulse-heating provides access to a wide range of thermophysical data (such as normal spectral emittance, specific enthalpy, electrical resistivity, isobaric heat capacity, thermal conductivity, and thermal diffusivity) in the solid and liquid states, which may not be accessible by levitation. Similar to the DLR experiment, pyrometric temperature assignment based on the recorded surface radiance and the use of Planck's radiation law is used throughout.

Density measurements are an addition to the standard measurement procedure of a regular pulse-heating experiment and thus require additional optical elements, but can be carried out simultaneously without further limitations. The sample is backlit with a strong light-source (flash) and the optically magnified shadowgraph imaged onto a CCD chip deploying a channel plate as a shutter. Most of the CCD chip is masked leaving exactly 16 lines of the photosensitive area open for exposure.[2] After exposure, the content of these 16 lines is transfered to the masked, and thus unexposed, area of the chip by shifting lines. Using the rest of the chip for data storage takes less time than actually reading the lines' content into a PC. A total of 36 consecutive cycles of exposure and shifting can be performed with the system until the CCD chip is 'full' and the content recorded. Slightly dependent on the actual exposure time, a typical exposure-shift cycle takes about 4.9 μs, yielding 10–12 images of the small sample area during a typical experiment of about 60 μs. If the initial sample diameter is known, the sample's cross-sectional expansion (ratioed to its diameter at room temperature) is a measure of the overall thermal expansion. Finally, the temperature-dependent density is obtained from the density at room temperature and the previously mentioned thermal expansion ratio. For an example of the image captured by the expansion systems, readers are directed to our second contribution to the TEMPMEKO 2007 proceedings [5].

The electrical resistivity is straightforwardly obtained from the current through the sample, I, and the voltage drop across a defined length of the sample, U, whose time dependences (together with the sample's surface radiance) are continuously recorded during the pulse-heating experiment. Initially, this yields electrical resistivity for the initial geometry. The results need to be corrected for the sample's volumetric expansion to obtain electrical resistivity. More detailed information can be found in Refs. [6] and [7].

[2] Accordingly, only the small fraction of the sample's shadowgraph corresponding to these 16 lines is monitored and recorded.

Table 1 Compiled specimen properties for CuNi-alloys and pure metals

Material	Supplier	T_m / T_l(K)	Density at RT(kg·m^{-3})
DLR			
Cu60Ni40	DLR[a]	1553 [4]	–
Cu50Ni50	DLR[a]	1593 [4]	–
Cu	DLR[a]	1357.77 [8]	–
Ni	DLR[a]	1728 [9]	–
TUG			
Cu53Ni47	Alfa Aesar	1573 [10]	8900[b]
Cu	Advent Research Materials, Ltd.	1357.77 [8]	8935 [11]
Ni	Advent Research Materials, Ltd.	1728 [9]	8907 [11]

Alloy compositions are given in at%; T_m / T_l is the melting/liquidus temperature for the metals/alloys; densities are given at room temperature as used for calculations at TUG
[a]DLR alloyed their sample materials from raw materials
[b]The density for constantan was measured by accurately weighing a larger sample

2.3 Specimens

Different specimens were used for the levitation and pulse-heating experiments. While DLR produced their own samples from pure copper and nickel, TUG purchased commercially available wire-shaped specimens from Advent Research Materials, Ltd. (copper: #B/1, 99.996% purity, and nickel: #Gi1136, 99.98% purity) and Alfa Aesar (Cu55–Ni45).

The samples used for the levitation experiments were typically spherically shaped, with a diameter of 5 mm. Besides the two pure metals, DLR managed to produce and measure the following binary Cu–Ni alloys[3] (in at%): Cu90Ni10, Cu80Ni20, Cu60Ni40, Cu50Ni50, Cu30Ni70, and Cu10Ni90 for density and Cu80Ni20, Cu60Ni40, Cu40Ni60, and Cu20Ni80 for resistivity.

The wire-shaped pulse-heating samples were nominally 0.5 mm in diameter and typically 60 mm in length. Due to limited technical use, only a Cu55Ni45 (in mass%)[4] alloy, commonly known as constantan®, was commercially available, having the same geometry as the pure metals. A compilation of relevant material properties for all specimens is presented in Table 1.

2.4 Procedures

2.4.1 Density

Density data with DLR's levitation setup are obtained from the optically detected circumference of the drop (yielding its volume—assuming spherical geometry) given that the mass of the sample is known and remains constant throughout the experiment. This assumption can be checked by weighing the sample before and after the

[3] With the possible exception near room temperatures, copper and nickel are totally miscible in the molten state [10].

[4] Equivalent to Cu53Ni47 (in at%), for better comparison to DLR measurements.

experiment. Typically, temperature-dependent density data, $d(T)$, are well represented by linear fits of the type

$$d(T) = d_l + d_T(T - T_l) \tag{1}$$

with d_l and d_T representing, respectively, the density at the liquidus temperature, T_l, and the thermal expansion coefficient.

The expansion measurement at TUG yields temperature-dependent data for the increase in diameter (or radius) by ratioing to the known diameter at room temperature (RT). Given that the length of the pulse-heated sample is constant throughout the experiment (which was shown experimentally, see Refs. [12] and [13]), this information can be linked to the volume expansion ratio $V(T)/V_0$ with $V(T)$ being the actual volume and V_0 the volume at RT. Finally, the temperature-dependent density is obtained from the knowledge of the density at RT, d_0, by

$$d(T) = d_0 \frac{V_0}{V(T)} \tag{2}$$

It has to be noted that $V(T)/V_0$ in the liquid state is expected, and thus calculated, to be a linear function of temperature. In turn, the result from Eq. (2) is mathematically a rational function and no longer linear. In most cases this deviation from linear behavior is negligible compared to the overall uncertainty, and therefore linear fits will be given for the results within this work, thereby omitting the small nonlinear effects.

2.4.2 Electrical Resistivity

At DLR, the electrical resistivity is obtained from measurements of the absolute values of current (in the primary coil) and the induced voltage (in the secondary coil) of the transformer as well as their phase difference, yielding the complex impedance, Z. Consequently, electrical resistivity, $\rho(T)$, is calculated from the theoretical correlation between $Z(T)$ and $\rho(T)$. Please refer to Refs. [3] and [4] for more details.

In order to employ Ohm's law for the pulse-heating setup at TUG, the current through the specimen and the voltage drop across it are recorded directly, yielding electrical resistivity for the initial geometry (not accounting for thermal expansion), $\rho_{IG}(T)$. In a second step, the electrical resistivity, corrected for the thermal (volume) expansion[5], $\rho(T)$, is obtained by

$$\rho(T) = \rho_{\mathrm{IG}}(T) \frac{V(T)}{V_0}. \tag{3}$$

2.4.3 Uncertainties

Still missing is an elaboration of the uncertainty budget for the newly remodeled expansion system at TUG according to standard best practice guides, like the GUM

[5] In other publications of our group also referred to as ρ_{VE}

[14]. These calculations are underway and until their completion only 'best estimates' will be presented in this manuscript. For now, an expanded standard uncertainty of $< 6\%$ is estimated for the density in the liquid state. Combining the expanded uncertainty for the liquid state electrical resistivity with the initial geometry ($\pm 2\%$) with the uncertainty for density leads to a 'best estimate' for electrical resistivity of about $\pm 8\%$. No such estimate is yet given for the levitation setup at DLR, but the development of an uncertainty budget is planned.

3 Results

3.1 Density

The comparison of experimental density data for CuNi-alloys and the respective pure constituents are given in Figs. 1–3. Since the commercially available Cu55Ni45 alloy measured at TUG did not match the composition of any of DLR's samples, the closest two alloys (composition-wise) are shown instead in Fig. 1. It can be seen from the same figure that the density obtained with the pulse-heating experiment seems to be higher than DLR's measurements, an effect that is systematically observed for all measurements reported in this manuscript. This effect might be partially due to different specimen materials and/or a consequence of differences in RT densities.[6] Furthermore, a combination of less thermal expansion under such high heating rates (compared to quasi-static measurements) and an overall non-uniform expansion (direction-wise, more radial than axial expansion) are currently investigated as sources for this effect of systematically larger densities at TUG. A consistent and more elaborate explanation is currently being sought. Despite the density differences at the liquidus, it can be seen that the temperature-dependencies (slopes) of the densities of Cu60Ni40 and constantan are in good agreement, and all density values agree within the estimated uncertainties.

The findings for the densities of pure copper and nickel as presented in Figs. 2 and 3 are similar to the results for the alloys. Measurements by pulse-heating predict higher densities in the liquid state than the levitation results, while the slopes (temperature dependences) are in reasonable agreement. To provide further comparison, literature data from Lucas [15], obtained with the maximum bubble pressure method, have also been added. For liquid copper (Fig. 2), Lucas' data are close to the mean of DLR's and TUG's density data, whereas for liquid nickel (Fig. 3), the literature data are even lower than the levitation results. Considering the difficulties and challenges presented by liquid metals, a larger uncertainty should be expected within which the presented results may be considered as being in reasonable agreement.

[6] As explained in Sect. 2.4 (Procedures), density measurements at TUG depend on knowledge of the RT density of the specimen material.

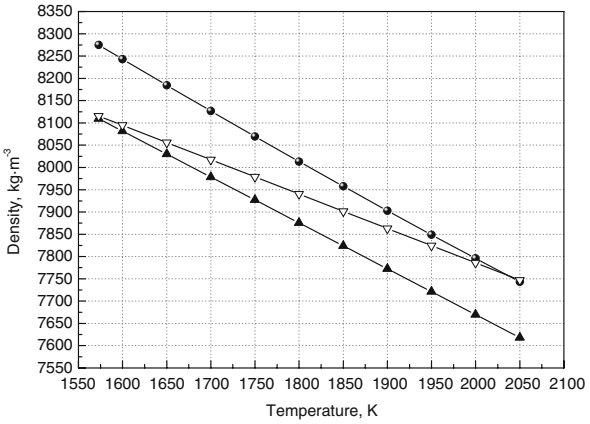

Fig. 1 Density of Cu53Ni47 and similar alloys (in the vicinity of the constantan composition) in the liquid state. Circles: Cu53Ni47 at TUG; up-triangles: Cu60Ni40 at DLR; open down-triangles: Cu50Ni50 at DLR. All compositions are given in at%

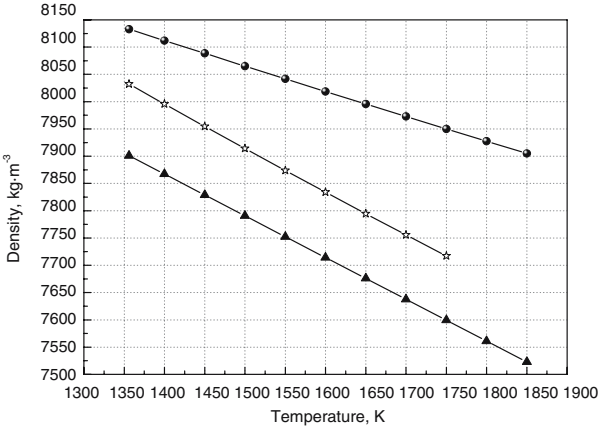

Fig. 2 Density of liquid copper as a function of temperature. Circles: TUG; up-triangles: DLR; stars: data from Ref. [15]

3.2 Electrical Resistivity

Electrical resistivity results for all the investigated materials are presented in Figs. 4–6, once again starting with the alloy (Fig. 4) followed by pure copper (Fig. 5) and then pure nickel (Fig. 6). For the CuNi-alloys, it has to be noted that (unlike the density results) Cu40Ni60 was measured by DLR instead of Cu50Ni50, in addition to Cu60Ni40. At the liquidus temperature, the TUG data for constantan are almost the mean of the two CuNi-alloys measured at DLR. The trend in the liquid phase shows good agreement for Cu40Ni60, but an interesting crossing-over for Cu60Ni40. However, by interpolating DLR's results to the constantan mixing ratio, a decent overlap within the stated uncertainties is achieved.

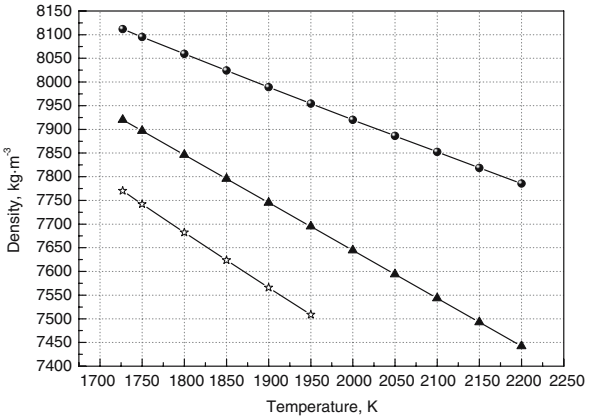

Fig. 3 Density of liquid nickel as a function of temperature. Circles: TUG; up-triangles: DLR; stars: data from Ref. [15]

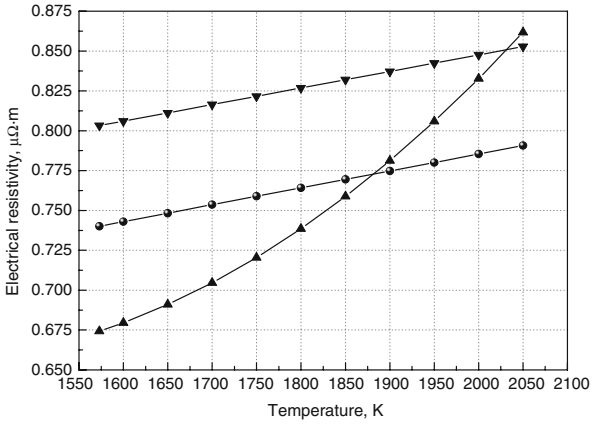

Fig. 4 Electrical resistivity of Cu53Ni47 and similar alloys (in the vicinity of the constantan composition) in the liquid state. Circles: Cu53Ni47 at TUG; up-triangles: Cu60Ni40 at DLR; open down-triangles: Cu40Ni60 at DLR. All compositions are given in at%

For pure copper, this agreement becomes even better as the levitation and pulse-heating data show a small discrepancy (less than 2%) at the melting temperature, but almost match at the maximum investigation temperature. By comparison, the literature results from Matula [16] for liquid copper differ only slightly from DLR's data. A possible explanation for the excellent agreement in resistivity for pure copper might be the high quality and reproducibility of the samples, even if the material originates from different suppliers and/or batches. Finally, the experimental results for the resistivity of pure nickel are shown in Fig. 6. Unlike the case for copper, the initial observed difference at the melting temperature (about 2.8%) increases with temperature to about 9% at the highest reported temperature. For nickel, the pulse-heating data from TUG are lower than DLR's, which might be partially due to the density differences as reported in Fig. 3. Liquid-state resistivity data from Seydel and Fucke [17] are also presented

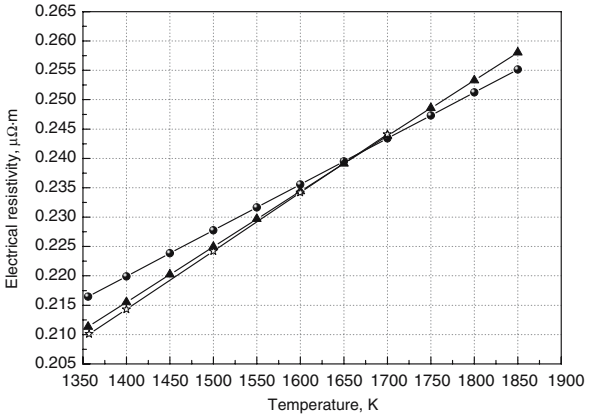

Fig. 5 Temperature-dependent electrical resistivity of liquid copper. Circles: TUG; up-triangles: DLR; stars: data from Ref. [16]

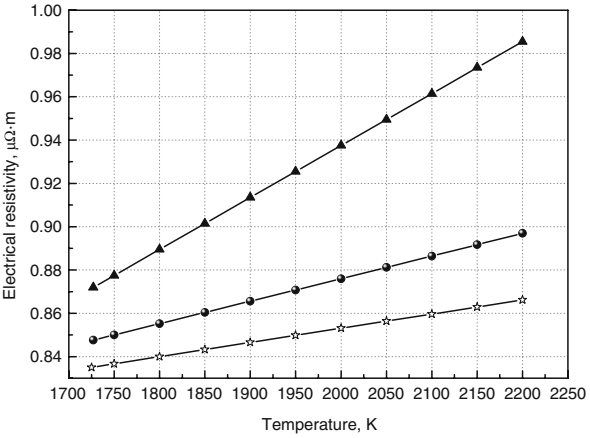

Fig. 6 Temperature-dependent electrical resistivity of liquid nickel. Circles: TUG; up-triangles: DLR; stars: data from Ref. [17]

in Fig. 6. Though these data are even lower than the pulse-heating results presented in this manuscript, they resemble more the TUG values than DLR's results. Seydel and Fucke also obtained their data with a resistive pulse-heating setup, but under elevated pressure (possibly counteracting or even suppressing thermal expansion and thus leading to smaller resistivity values).

The summarized density and electrical resistivity data from this manuscript can be found in Table 2.

4 Conclusions

The measurements reported here are the first step in a comparison project to obtain density and electrical resistivity data for liquid metals and alloys with two completely

Table 2 Density and electrical resistivity data for CuNi-alloys and pure metals

Institution	Material	T_m/T_l[a](K)	$d_{m/l}$(kg·m^{-3})	d_T (kg·m^{-3}· K^{-1})
Density, $d(T) = d_{m/l} + d_T(T - T_{m/l})$				
	Cu60Ni40	1553	8130	−1.030
DLR	Cu50Ni50	1593	8100	−0.772
	Cu	1357	7900	−0.765
	Ni	1728	7920	−1.010
	Cu53Ni47	1573	8275	−1.115
TUG	Cu	1357	8133	0.462
	Ni	1728	8112	−0.691
Institution	Material	$\rho_0(\mu\Omega\cdot m)$	$\rho_1(\mu\Omega \cdot m \cdot K^{-1})$	$\rho_2(\mu\Omega \cdot m \cdot K^{-2})$
Electrical resistivity, $\rho(T) = \rho_0 + \rho_1 T + \rho_2 T^2$				
	Cu60Ni40	147.52×10^{-2}	-1.20×10^{-3}	4.40×10^{-7}
DLR	Cu40Ni60	63.96×10^{-2}	1.04×10^{-4}	0
	Cu	8.32×10^{-2}	9.45×10^{-5}	0
	Ni	45.75×10^{-2}	2.40×10^{-4}	0
	Cu53Ni47	57.35×10^{-2}	1.06×10^{-4}	0
TUG	Cu	11.03×10^{-2}	7.83×10^{-5}	0
	Ni	66.76×10^{-2}	1.04×10^{-4}	0

Alloy compositions are given in at%; T_m/T_l is the melting/liquidus temperature for the metals/alloys, $d_{m/l}$ is the density at melting/liquidus, d_T represents the thermal expansion coefficient, and ρ_0 to ρ_2 are the fit parameters for electrical resistivity. All polynomials are valid from melting/liquidus to about 400 K in the liquid state

[a] T_m applies to pure metals, T_l to alloys

different techniques, namely electromagnetic levitation at DLR and resistive pulse-heating at TUG. Results for the binary CuNi-alloy (similar to constantan) and its pure constituents show reasonable agreement within preliminary estimated uncertainties. A rigorous uncertainty budget for both techniques is planned, but yet to be undertaken. Nevertheless, the first comparisons of the data exhibit some interesting systematic differences in both techniques which need to be further investigated and addressed.

Acknowledgments This project is sponsored by Österreichische Forschungsförderungsgesellschaft mbH (FFG) and Österreichisches Weltraumprogramm (ASAP), Vienna, Austria.

References

1. I. Egry, G. Lohöfer, I. Seyhan, S. Schneider, B. Feuerbach, Int. J. Thermophys. **20**, 1005 (1999)
2. G. Lohöfer, J. Piller, The new ISS electromagnetic levitation facility: MSL – EML, *Proceedings of 40th AIAA Aerospace Sciences Meeting & Exhibit*, AIAA 2002–0764 (2002)
3. T. Richardsen, G. Lohöfer, I. Egry, Int. J. Thermophys. **23**, 1207 (2002)
4. G. Lohöfer, J. Brillo, I. Egry, Int. J. Thermophys. **25**, 1535 (2004)
5. B. Wilthan, H. Reschab, R. Tanzer, W. Schützenhöfer, G. Pottlacher, in Proc. TEMPMEKO 2007 (to be published in Int. J. Thermophys.)
6. B. Wilthan, C. Cagran, C. Brunner, G. Pottlacher, Thermochim. Acta **415**, 47 (2004)
7. M. Boivineau, G. Pottlacher, Int. J. Mater. Prod. Technol. **26**, 217 (2006)
8. H. Preston-Thomas, Metrologia **27**, 3 (1990)
9. R.E. Bedford, G. Bonnier, H. Maas, F. Pavese, Metrologia **33**, 133 (1996)

10. E.A. Feest, R. D. Doherty, J. Inst. Metals **99**, 102 (1971)
11. J.W. Arblaster, Private communication, Coleshill Laboratories, Gorsey Lane, Coleshill, West Midlands B46 1JU, UK (2007)
12. V.M. Kul'gavchuck, G.A. Novoskol'tseva, Sov. Phys. Tech. Phys. **11**, 406 (1966)
13. K.W. Henry, D.R. Stephens, D.J. Steinberg, E.B. Boyce, Rev. Sci. Instrum. **43**, 1777 (1972)
14. Expression of the Uncertainty of Measurement in Calibration, EA-4/02, http://www.european-accreditation.org/n1/doc/ea-4–02.pdf
15. L.-D. Lucas, in Viscometry and Densitometry, ed. by R.A. Rapp. Physcichemical Measurements in Metals Research, vol. IV–Part 2, (Interscience Pubs., New York, 1970), pp. 219–292
16. R.A. Matula, J. Phys. Chem. Ref. Data **8**, 1147 (1979)
17. U. Seydel, W. Fucke, Z. Naturforsch. **32a**, 994 (1977)